CFD MODELLING OF RADIATIVE HEAT TRANSFER OF AN IN-HOUSE HELIUM STABILIZED, LAMINAR PREMIXED FLAT FLAME

Haider S.[a], Ivarsson A.[a], Pang K.M.[a,*], Schramm J.[a], Mansouri S.H.[b]
*Author for correspondence
[a]Department of Mechanical Engineering,
Technical University of Denmark,
Nils Koppels Allé, Kgs. Lyngby, 2800,
Denmark,
[b]Department of Mechanical Engineering,
Shahid Bahonar University of Kerman,
P. O. Box 76175-133, Kerman,
Iran,
E-mail: kmpan@mek.dtu.dk

ABSTRACT

The current work describes a multi-dimensional Computational Fluid Dynamics study of an in-house helium stabilized, laminar premixed flat flame, with an emphasis on the radiation modelling. The experimental work first deals with the post flame instability induced by the difference of gas densities at the downstream and upstream of the flat flame. A non-intrusive method which is addressed as helium stabilization is developed, where helium enters the chamber as a co-flow jet to dilute the combustion products and hence minimize the difference of gas densities between downstream and upstream of the flame. A thermometry method based on infrared emission and absorption by carbon dioxide between 2100 and 2400 cm^{-1} is then applied for temperature measurement. In the numerical efforts, a sooting flame with an equivalence ratio value of 2.15 is simulated. The associated experimental temperature and soot volume fraction profiles at different heights along the axial direction are used to validate a local time stepping (LTS) based solver. Radiation of the both gas and soot is taken into account. For the gas phase species, a Wide Band Box model is incorporated into the solver to account for thermal radiation from CO_2 and H_2O and the model parameters are calculated using HITRAN2012 radiation database. On the other hand, the soot absorption coefficient is calculated using the relation based on the associated soot volume fraction and local cell temperature. Results generated using the Weighted Sum of Gray Gases (WSGG) model are also included for comparison purposes. The temperature profile calculated using the Wide Band Box model is found closer to the measurements, as compared to those predicted using the WSGG model. The soot volume fraction calculated by the former are also closer to the measurement for the first 30 mm from the burner exit but both models overestimate the soot volume fraction at a further downstream location. The current results showed that the LTS solver predict the temperature and soot volume fraction of the stabilized, laminar premixed flames reasonably well. The solver can be used to examine more comprehensive yet computational expensive radiation submodels.

NOMENCLATURES

a, a_o	absorption coefficient, reaction order, soot model constant
b	reaction order, soot model constant
c	soot concentration
C_N, C_S	soot model constant
f	linear branching coefficient
f_c	mass fraction of carbon in the fuel material
g	linear termination coefficient
g_0	coefficient of linear termination of radical nuclei on soot particles
I_η, $I_{b\eta}$	local spectral intensity, blackbody spectral intensity
m_p	mass of soot particle
n_0	spontaneous formation of radical nuclei from the fuel
N_A	Avogadro number
p_{CO2}, p_{H2O}	partial pressures of CO_2 and H_2O
P	pressure
S	band intensity
$S_{nuclei,f}$, $S_{soot,f}$	source term for formation of nuclei and soot
$S_{nuclei,c}$, $S_{soot,c}$	source term for combustion of nuclei and soot
r	position
s	direction
t	time
T, T_a	local temperature, activation temperature
X_N	specific concentration of radical nuclei
Y_{fuel} , Y_S	mass fraction of fuel, mass fraction of soot

Greek symbols

Γ	diffusive coefficient
$\boldsymbol{\kappa}$	absorption coefficient
ρ	fluid density
ω_e	effective band width

Abbreviations

CFD	computational fluid dynamics
DOM	Discrete Ordinate Method
LTS	local time stepping
OpenFOAM	Open Field Operation and Manipulation
RTE	radiative transport equation
SVF	soot volume fraction
WSGG	Weighted Sum of Gray Gases

INTRODUCTION

Since the past decades, various premixed flame experiments have been carried out to study the associated fundamental features [1]. This flame type is of main interest due to its simplicity as the interaction with turbulence and the diffusion

between the fuel and air do not exist. However, evolution of the soot particles i.e. competition between soot formation and oxidation as well as radiation in this type of flame are still among the challenging topics. In parallel to the experimental development, one-dimensional model [2], for instance the PREMIX code is executively designed to compute species concentration and temperature profiles of steady state burner-stabilized and freely propagating laminar flames. This is useful to study chemical kinetics of various hydrocarbon fuels and the associated transport properties in a cost-effective manner. On the other hand, multi-dimensional computational fluid dynamics (CFD) simulations have also been used to couple the flow, chemical kinetics, radiation and soot models. In terms of radiation modelling, discrete ordinate method (DOM) is applied to solve the radiative transport equation (RTE). The radiation submodels for species absorption/emission and their respective effects on the overall heat transfer modelling are also studied. In addition to this, multi-step soot models can be implemented to predict the soot formation and oxidation processes. The temporal and spatial evolution of soot particles and the associated size growth have a great influence to the overall radiative heat transfer event, vice-versa.

In recent years, Open Field Operation and Manipulation (OpenFOAM) [3] code has been gaining great attention amongst CFD community due to its open-source feature which facilitates modification of the standard release code and also the integration of new models. This allows sharing within both the academia and industrial community. Although various researchers have developed different reacting flow solvers on this platform for their respective applications, its implementation for radiation modelling remains limited. The standard radiation library in OpenFOAM provides P1 [4] and finite volume DOM [5],[6] for the solution of RTE. For modelling the absorption/emission of participating species, a narrow band model [7] and a simple wide band model are available. Unfortunately, these models are not widely validated. In heat transfer applications, implementation of band models in the prediction of total emission and absorption is more desirable over the use of an entire band [4]. Calculation of band emission/absorption using line-by-line and narrow band models is computationally very expensive [8]. The computational cost further escalates when simulations is coupled with fluid flow and chemical kinetics.

In the current work, a Wide Band Box model is implemented into the OpenFOAM library. Its validity is examined using experimental data of an in-house, helium stabilized laminar premixed flat flame [9]. Measurements of a sooting flame are used. The main advantage of the current setup is that soot formation overwhelms soot oxidation and the latter can be neglected in the simulation. A description of the experimental setup is given in the next section. It is then followed by the model formulation, with an emphasis on the soot and radiation models. Subsequently, results and discussions are presented. The final section presents the main conclusion of this work.

EXPERIMENTAL SETUP

Figure 1 illustrates the in-house experimental setup. The flat flame burner used in the current experiment is the standard bronze McKenna burner. The work firstly deals with the post flame instability induced by the difference of gas densities at the downstream and upstream of the laminar premixed flat flame. A non-intrusive method which is addressed as helium stabilization is developed. The working principle of helium stabilization is equalizing the gas densities by diluting the surrounding gas at the downstream of the flame with helium. To achieve this, the experimental setup is designed such that the premixed fuel/air charge entered the combustion chamber through the center inlet while the helium gas entered as a co-flow jet at a low velocity. As the combustion chamber is filled with helium, the soot oxidant, oxygen is flushed off and soot oxidation can be omitted.

The stabilized flame is uniform and highly lifted. These features are appropriate for optical line of sight diagnostics in both pre- and post-combustion regions. Temperature and soot volume fraction along the axial direction up to the height of 150 mm above the burner surface are measured in the experiment. A thermometry method based on infra-red emission and absorption by carbon dioxide (CO_2) between 2100 and 2400 cm^{-1} is developed for temperature measurement of the premixed flat flame. The detection is performed with a Nicolet 6700 Fourier transform infra-red spectrometer. With the proper installation and measurement procedure, the method is capable to detect the temperature of the flame core within the precision of +/- 1 %, in spite of the line of sight principle. On the other hand, the light transmission method is used to measure the soot concentration given in terms of soot volume fraction. The transmission of visible light is measured using the combination of an Ocean Optics USB4000 VIS-NIR spectrometer, a green light-emitting diode light source, quartz lenses and quartz windows. Premixed flames formed by various fuel types at wide ranges of equivalent ratio are investigated in the experiment. The flames with different equivalence ratios are produced by controlling the flow rate of fuel and air utilizing a Hovagas G6 gas mixer. A more detailed description of the experimental setup and temperature/soot volume fraction measurements can be found in [9].

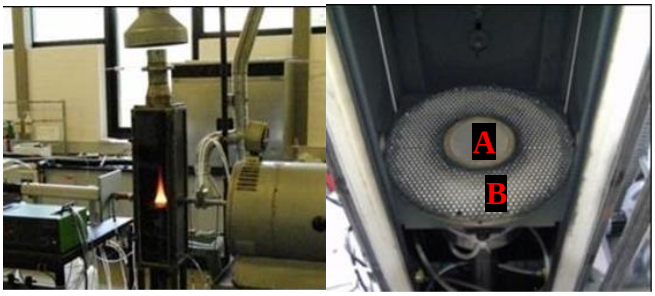

Figure 1 Front view of the combustion chamber (left) and top view of the McKenna burner where A is the premixed charge inlet while B is the helium co-flow (right)

NUMERICAL METHOD

Development of the solver and the performance benchmarking exercise in this work are carried out using OpenFOAM version 2.0.x. Figure 2 depicts the reflected 4-degree sector computational grid. This domain is used to represent a section of the combustion chamber used for the laminar premixed flame experiments as shown in Figure 1(a). Based on the mesh sensitivity analysis, fine mesh resolution is required at the regimes above the premixed charge inlet in the flow direction in order to deal with the high species and temperature gradients along the combustion process. As such, the smallest mesh size at the axial direction is set to 0.01 mm. This mesh configuration is found sensitive to predict the change of laminar flame speed and hence the heat loss and flame temperature near the burner surface when the pre-exponential factor is varied. The final computational grid consists of 114k cells. Further refinement in the spatial resolution does not further improve the results. Similar to the experimental setup, the grid accounted for two inlets. The premixed charge of ethylene fuel and air enters the domain through the inlet at the center at a velocity of 0.135 m/s. In the presented case, the inlet gas has a composition of ethylene, O_2 and N_2 with mass fraction of 0.1282, 0.2031 and 0.6687, respectively. Helium gas flows into the domain as a co-flow at a low velocity of 0.048 m/s. The domain also accounts for an internal wall such that the helium gas can be trapped to stabilize the flame.

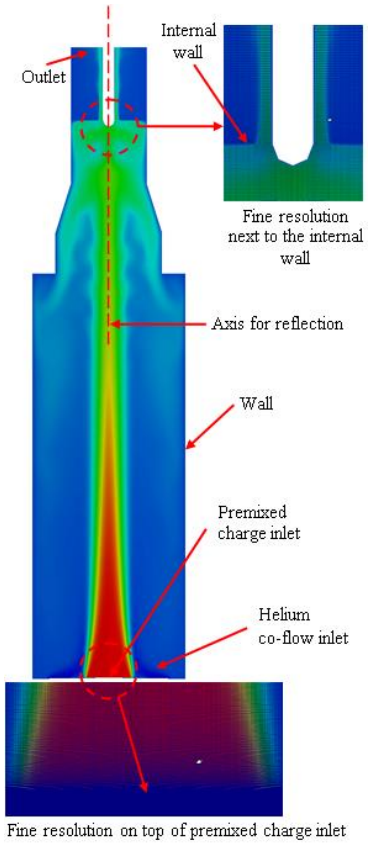

Figure 2 2-D computational domain of the combustion chamber

A Local Time Stepping (LTS) based solver is used to increase the computational efficiency. More detailed descriptions of the mesh configuration, boundary conditions, LTS model formulation can be found in [10]. By taking the advantage that chemical equilibrium is reached in the current case, a customized global, irreversible chemical reaction, $5C_2H_4+7O_2 \rightarrow 9CO+CO_2+7H_2+3H_2O$ is applied. A simplification on the formulation soot model is also allowed, as presented next.

Magnussen Soot Model

The Magnussen model [11] is used whereby two transport equations as described by Equations (1) and (2) are solved for the specific concentration of radical nuclei, X_N and the soot mass fraction, Y_S, respectively.

$$\frac{\partial \rho X_N}{\partial t} + \nabla \cdot (\rho \vec{v} X_N) = \nabla \cdot (\mu \nabla X_N) + S_{nuclei,f} + S_{nuclei,c} \quad (1)$$

$$\frac{\partial \rho Y_S}{\partial t} + \nabla \cdot (\rho \vec{v} Y_S) = \nabla \cdot (\mu \nabla Y_S) + S_{soot,f} + S_{soot,c} \quad (2)$$

X_N can be interpreted in the form of number of soot particles per unit volume, N while Y_S can be used to calculate the soot volume fraction, f_v. The latter are then compared against the experimental data. This concept resembles that of other multi-step soot models proposed by Leung and Lindstedt model [12] and Moss et al. [13] which implement the similar transport equations. In other words, only different soot formation and oxidation submodels are used to define the source term. Here, the source terms for formation of nuclei, $S_{nuclei,f}$ and soot, $S_{soot,f}$ are calculated using the empirical models of Tesner et al. [14] as shown below,

$$S_{nuclei,f} = n_0 + (f - g)C_N - g_0 C_N C_S \quad (3)$$

$$S_{soot,f} = m_p (a - bC_S) C_N \quad (4)$$

In Equation (3), f and g denote the linear branching coefficient and the linear termination coefficient, respectively. g_0 is the coefficient of linear termination of radical nuclei on soot particles. The remaining soot model parameters are calculated as follows,

$$n_0 = a_0 Y_{fuel} f_c \exp\left(\frac{-T_{a,0}}{T}\right) \quad (5)$$

$$C_N = \rho N_A X_N \quad (6)$$

$$C_S = \rho \frac{Y_S}{m_p} \quad (7)$$

n_0 is defined as the spontaneous formation of radical nuclei from the fuel. It is modelled based on the Arrhenius expression and is fuel dependent. Y_{fuel} denotes the mass fraction of fuel while f_c is the mass fraction of carbon in the fuel material which is set as 24/26. $T_{a,0}$ represents the activation temperature here. N_A in Equation (6) is the Avogadro number. Lastly, the m_p in Equation (7) is the mass of soot particle. As aforementioned,

the premixed flame is surrounded by inert gas, helium. Soot oxidation is hence negligible. Source terms for combustion of nuclei, $S_{nuclei,c}$ and soot, $S_{soot,c}$ are set to zero. Soot model parameters are calibrated to reproduce the experimental soot amount. The model constant values implemented are summarized in Table 1.

Table 1 Soot model parameters calibrated to achieve the measured soot volume fractions

Model parameters		
a_0	3.32 x 10^{14}	mol/kg/s
$T_{a,0}$	83000	K
$(f\text{-}g)$	100	1/s
g_0	1.63 x 10^{10}	m^3/mol/s
a	1 x 10^5	1/s
b	4.82 x 10^{10}	m^3/mol/s

Wide Band Box Radiation Model

In this section, the model description focuses on the RTE and the Wide Band Box model which is integrated to the submodel library. For an absorbing, emitting and non-scattering medium at position $\vec{r}$ and direction $\vec{s}$, the RTE is given as

$$\frac{dI_\eta(\vec{r},\vec{s})}{ds} = -\kappa_\eta I_\eta(\vec{r},\vec{s}) + \kappa_\eta I_{b\eta}(\vec{r},\vec{s}) \quad (9)$$

where I_η and $I_{b\eta}$ represent the local and blackbody spectral intensity, respectively. κ_η represents the spectral absorption coefficient of participating species. This equation describes the rate of change of radiation intensity at position $\vec{r}$ along the path ds and in the direction $\vec{s}$. The RTE is solved using DOM along 64 ordinates in the current work. The DOM requires the absorption coefficient as an input. In current case, CO_2, H_2O and soot are considered to be the participating species. The absorption coefficients for CO_2, H_2O are calculated using the spectral Wide Band Box model.

The box or 'top-hat' model proposed by Penner [15] is the simplest wide band model. It approximates a given band with a rectangular box. The width of the band is calculated as 'effective band width', $\Delta\omega_e$ and the height of the band is determined by a mean absorption coefficient, $\bar{\kappa}$. For a given band, 'i', the mean absorption coefficient is assumed to be constant in the given band and is related to band intensity by

$$\bar{\kappa}_i = \frac{S_i}{\Delta\omega_{e_i}} \quad (10)$$

The band intensity can be calculated as

$$S_i = \int_{band} \kappa_\eta \, d\eta \quad (11)$$

For a gas mixture of H_2O and CO_2, the absorption coefficient of the mixture is obtained by simply adding the absorption coefficients of the individual species.

$$\bar{\kappa}_{\eta,g\ i} = \bar{\kappa}_{\eta,H_2O_i}\, p_{H_2O} + \bar{\kappa}_{\eta,CO_2\ i}\, p_{CO_2} \quad (12)$$

where p represents the partial pressure of each specie. The radiation model access the concentration of each participating species directly from the reacting flow solver. In addition to this, the band overlap error is also taken into consideration in the current Wide Band Box model. Modest [4] as well as Liu and Zhang [16] used exponential Wide Band model and first law of quantum mechanics, respectively to calculate the band mean absorption coefficients for a given species in their simulations. The current study proposes new polynomial relations to calculate the mean absorption coefficient of H_2O and CO_2 in a given band. The polynomial relations are developed by calculating the absorption coefficients of H_2O and CO_2 from latest edition of spectral radiation database HITRAN2012. For each gaseous specie and a given band, the calculations are carried out for mole fraction of 1.0 and at temperatures of 300 K, 600 K, 1000 K, 1500 K, 2000 K and 2500 K. A polynomial data fitting is then conducted. Polynomial coefficients for both H_2O and CO_2 can be found in Table 2.

$$\bar{\kappa}_{\eta,g\ i} = c_0 + c_1 T + c_2 T^2 + c_3 T^3 \quad (13)$$

Table 2 Absorption coefficients for the Wide Band Box Model

	Band, μm			
	2.5-3.0	4.0-4.65	4.8-8.0	12.5-25.0
CO_2				
c_0	25	15.328		87.044
c_1	-2.232x10^{-2}	-1.6866		-0.13197
c_2	1.2416x10^{-5}	9.4148x10^{-4}		7.2501x10^{-5}
c_3	-2.3398x10^{-9}	-1.7557x10^{-7}		-1.3355x10^{-8}
H_2O				
c_0	44.53		48.843	-19.268
c_1	-6.762x10^{-2}		-7.324x10^{-2}	9.0457x10^{-2}
c_2	3.7529x10^{-5}		4.0495x10^{-5}	-5.3833x10^{-5}
c_3	-6.9523x10^{-9}		-7.5037x10^{-9}	9.1218x10^{-9}

Soot has a continuous spectrum and the radiative properties of soot depend on its concentration and distribution in the flame [17]. By considering that soot particle sizes are generally very small, these particles are assumed to be non-scattering and the soot absorption coefficient is taken in the Rayleigh scattering limit. In this study the soot absorption coefficient is calculated as [18].

$$\kappa_{\eta,soot} = 2370\, f_v T \quad (14)$$

Here, f_v and T denote the soot volume fraction and local temperature, respectively. The total spectral absorption coefficient for the gas-soot mixture is then calculated as [19]

$$\kappa_\eta = \bar{\kappa}_{\eta,g\ i} + \kappa_{\eta,soot} - \bar{\kappa}_{\eta,g\ i}\kappa_{\eta,soot} \quad (15)$$

COMPARISONS OF TEMPEATURARE AND SOOT VOLUME FRACTION PROFILES

Here, comparisons are made between the experimental measurement and simulated temperature profiles when different radiation modelling approaches are used. WSGG model results are extracted from the previous work [10]. The soot volume fraction recorded in the experiment is also used to evaluate the effects of temperature on soot formation. Figure 3 depicts the experimental and simulated temperature generated by WSGG and Wide Band Box models.

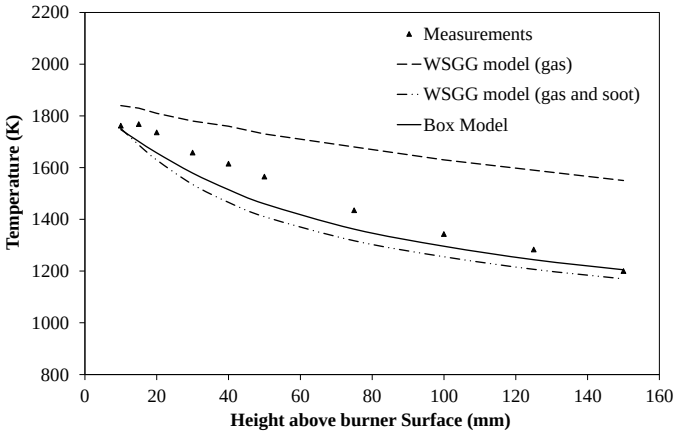

Figure 3 Comparisons of experimental measurement and simulated temperature profiles using different radiation models

In general, the drop of flame temperature at higher axial position is predicted by all the models. An evaluation of WSGG model shows that the use of fitting coefficients for gas-phase radiation is insufficient to capture the radiative heat loss of the rich and sooty flame. The prediction is improved by substituting the submodel with the model which incorporates soot radiation. The radiative heat loss is more significant and associated temperature profile is closer to the experimental measurement, suggesting the importance of soot radiation in this case. In case of WSGG model, the simulated results show steeper gradients i.e. the drop of temperature is greater. This could be attributed to the p_{H2O}/p_{CO2} ratio. The p_{H2O}/p_{CO2} ratio in the test case approximates 3 but the data set used here is meant for a ratio of 2. Further improvement is required by applying a more appropriate set of fitting coefficients for the radiation modelling of WSGG model. On the other hand, the Wide Band Box model is independent from the p_{H2O}/p_{CO2} ratio. The axial temperature predicted using the Wide Band Box model is consistently higher and closer to the measurement in case of Wide Band Box model. From the height of 120 mm to 150 mm, the Wide Band Box model predicts the temperature profile in good agreement with the measured values.

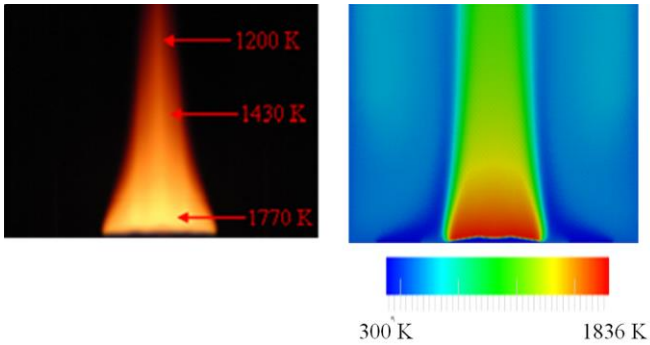

Figure 4 Comparisons of (a) experimental flame image against temperature contours [3] simulated by Wide Band Box Model

The temperature contours computed by Wide Band Box model are compared to the experimental flame image in Figure 4. As illustrated, the flame lift-off observed in the experiment is replicated using the current customized reaction. Replication of this feature is significant to produce the upstream temperature. Otherwise, with the use of the original pre-exponential factor, a high flame speed is produced and the associated flame transports nearer to the cold burner surface. The heat loss due to convection is high and hence the predicted flame temperature near the burner surface is lower. It is noteworthy that once the flame is lifted up, a further reduction of the value does not influence the flame temperature anymore. Also, when the value is too small, a low laminar flame speed is yielded and the flame does not stabilize but a flame "blow-off" phenomenon is observed [20].

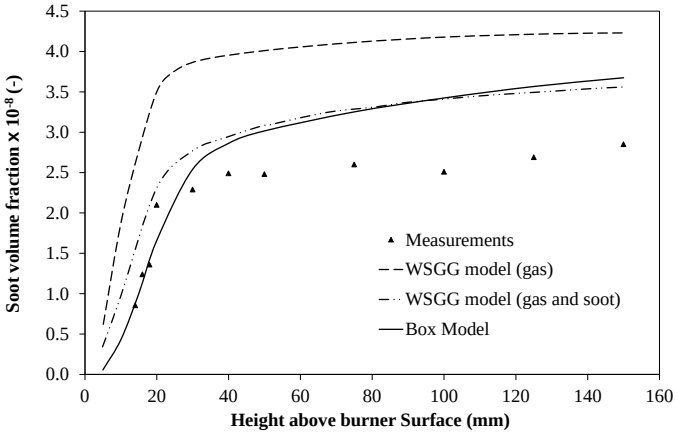

Figure 5 Comparisons of experimental measurement and simulated soot volume fraction profiles using different radiation models

Figure 5 illustrates the comparison of measured and simulated soot volume fraction. As demonstrated, the soot volume fraction calculated, with only gas-phase radiation is much greater as compared to the measurement. This is attributed to the inaccurate associated temperature prediction. At higher simulated local temperature, more soot is formed and an

overestimation of soot volume fraction is observed. The overall soot volume fraction prediction is improved when the soot radiation is considered by the WSGG model, particularly at the height of below 20 mm above the burner surface. It is however, overestimated when the height increases. Similar trend is also observed when the Wide Band Box model is implemented. Besides these, it is worth mentioning that a speedup of approximately fourteen-fold is achieved using the LTS based solved, as compared to the computational runtime required by the counterpart transient solver [10].

CONCLUSION

The current paper describes experimental and numerical investigation of the in-house helium stabilized, laminar premixed flat. The helium stabilization method is developed and successfully addresses the post flame instability induced by the difference of gas densities at the downstream and upstream of the flat flame. This facilitates the measurement of temperature and combustion product concentration. Also, due to the chemical equilibrium and absence of soot oxidation in this flame setup, simplifications can be carried out on the formulation of chemical and soot models. The focus can then be put on validation of the radiation model. A parametric study showed that soot radiation has great effects on the temperature and soot volume fraction predictions of the sooting flame. The temperature profile calculated using the Wide Band Box model is found closer to the measurements, as compared to those predicted using the Weighted Sum of Gray Gas model. The soot volume fraction calculated by the former are also closer to the measurement for the first 30 mm from the burner exit but both models overestimate the soot volume fraction at a further downstream location. The current solver has been proved to predict the temperature and soot volume fraction of the stabilized, laminar premixed flames reasonably well. With such expedited calculation, the local time stepping based solver is also seen as a useful tool to examine more comprehensive yet computational expensive radiation submodels.

ACKNOWLEDGEMENT

The authors acknowledge Innovation Fund Denmark and MAN Diesel & Turbo A/S for funding the RADIADE project. We are also grateful to Martin Becker from DHCAE Tools for sharing his experience of the implementation of the LTS solver.

REFERENCES

[1] L. Wang, D.C. Haworth, S.R. Turns, M.F. Modest, Interactions among soot, thermal radiation, and NOx emissions in oxygen-enriched turbulent nonpremixed flames: A computational fluid dynamics modeling study, Combust. Flame 141 (2005) 170-179.

[2] K.K. Kuo, Principle of Combustion, second ed., John Wiley & Sons Inc., New Jersey, 2005, pp. 210-215.

[3] H.G. Weller, G. Tabor, H. Jasak, C. Fureby, A tensorial approach to computational continuum mechanics using object-oriented techniques, Am. Inst. Phys. 12 (1998) 620-631.

[4] F.M. Modest, Radiative Heat Transfer, second ed., Academic Press, California, 2003, pp. 472.

[5] E. H. Chui and G. D. Raithby. , Computation of Radiant Heat Transfer on a Non-Orthogonal Mesh Using the Finite-Volume Method. Numerical Heat Transfer, Part B, 23:269-288, 1993.

[6] G. D. Raithby and E. H. Chui. ,A Finite-Volume Method for Predicting a Radiant Heat Transfer in Enclosures with Participating Media. J. Heat Transfer, 112:415-423, 1990.

[7] Barlow, R. S., Karpetis, A. N., Frank, J. H., and Chen, J.-Y., Sclar Profiles and NO formation in Laminar Opposed-Flow Partially Premixed Methane/ Air Flames. Combust. Flame 127:2102-2118 (2001).

[8] R. Viskanta, Radiative Transfer in Combustion Systems: Fundamentals and Applications, Begell House Inc, New York, 2005.

[9] A. Ivarsson, Modeling of heat release and emissions from droplet combustion of multi component fuels in compression ignition engines, PhD thesis, Technical University of Denmark, Lyngby, 2009.

[10] K.M. Pang, A. Ivarsson, S. Haider, J. Schramm, Development and validation of a local time stepping solver-based PaSR solver for combustion and radiation modeling, 8th OpenFoam Workshop, Jeju, South Korea, 2013.

[11] B.F. Magnussen, B.H. Hjertager, On mathematical modeling of turbulent combustion with special emphasis on soot formation and combustion, Symp. (Int.) Combust. 16 (1977) 719-729.

[12] K.M. Leung, R.P. Lindstedt, W.P. Jones, A simplified reaction mechanism for soot formation in nonpremixed flames, Combust. Flame 97 (1991) 289-305.

[13] S.J. Brookes, J.B. Moss, Predictions of soot and thermal radiation properties in confined turbulent jet diffusion flames, Combust. Flame 116 (1999) 486-503.

[14] P.A. Tesner, T.D. Smegiriova, V.G. Knorre V.G, Kinetics of dispersed carbon formation, Combust. Flame 17 (1971) 253-260.

[15] S.S. Penner, Quantitative Molecular Spectroscopy and Gas Emissivities, Addison-Wesley, Reading MA, 1960.

[16] Y. Liu and X. Zhang, Analysis of Gas Radiative Transfer Using Box Model and Its Comparison with Gray Band Approximation, Journal of Thermal Science. 12 (2003) 1.

[17] R. Seigel and J.R. Howell, Thermal Radiation Heat Transfer, Taylor and Francis , New York (2002).

[18] J.F. Widmann, Evaluation of the planck mean absorption coefficients for radiation transport through smoke, Combustion Science and Technology (2003) 175:12, 2299-2308.

[19] T.K. Bose, High Temperature Gas Dynamics: An Introduction for Physicists and Engineers, Springer, 2005.

[20] K.K. Kuo, Principle of Combustion, second ed., John Wiley & Sons Inc., New Jersey, 2005, pp. 507.